Elsevier Editorial System(tm) for Acta Biomaterialia

Manuscript Draft

Manuscript Number: AB-18-2210

Title: Tissue engineered hydrogels supporting 3D neural networks

Article Type: Full length article

Keywords: biosynthetic hydrogel; tissue engineering; supporting glia; neural networks; polyvinyl alcohol.

Corresponding Author: Dr. Ulises Alejandro Aregueta Robles, Ph.D.

Corresponding Author's Institution: University of New South Wales

First Author: Ulises Alejandro Aregueta Robles, Ph.D.

Order of Authors: Ulises Alejandro Aregueta Robles, Ph.D.; Penny J Martens, Ph.D.; Laura A Poole-Warren, Ph.D.; Rylie A Green, Ph.D.

Abstract: Promoting nerve regeneration requires engineering cellular carriers to physically and biochemically support neuronal growth into a long lasting functional tissue. This study systematically evaluated the capacity of a biosynthetic poly(vinyl alcohol) (PVA) hydrogel to support growth and differentiation of co-encapsulated neurons and glia. A significant challenge is to understand the role of the dynamic degradable hydrogel mechanical properties on expression of relevant cellular morphologies and function. It was hypothesised that a carrier with mechanical properties akin to neural tissue will provide glia with conditions to thrive, and that glia in turn will support neuronal survival and development. PVA co-polymerised with biological macromolecules sericin and gelatin (PVA-SG) and with tailored nerve tissue-like mechanical properties were used to encapsulate Schwann cells (SCs) alone and subsequently a co-culture of SCs and neural-like PC12s. SCs were encapsulated within two PVA-SG gel variants with initial compressive moduli of 16 kPa and 2 kPa, spanning a range of reported mechanical properties for neural tissues. Both hydrogels were shown to support cell viability and expression of extracellular matrix proteins, however, SCs grown within the PVA-SG with a higher initial modulus were observed to present with greater physiologically relevant morphologies and increased expression of extracellular matrix proteins. The higher modulus PVA-SG was subsequently shown to support development of neuronal networks when SCs were co-encapsulated with PC12s. The lower modulus hydrogel was unable to support effective development of neural networks. This study demonstrates the critical link between hydrogel properties and glial cell phenotype on development of functional neural tissues.

Research Data Related to this Submission

Title: Data for: Tissue engineered hydrogels supporting 3D neural networks
Repository: Mendeley Data
https://data.mendeley.com/datasets/gy6mcx73p7/draft?a=40c848a5-0e72-4428-ab3b-5584d2e18ada

Graphical Abstract

1

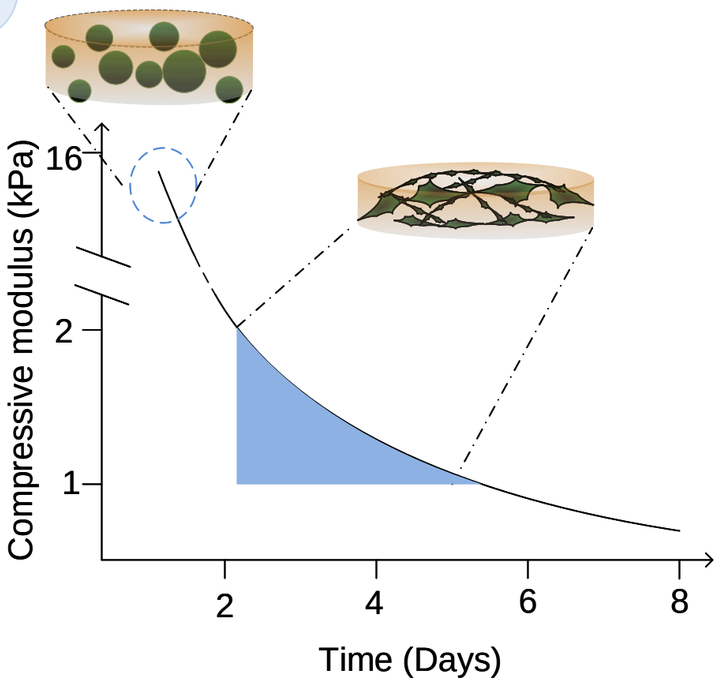

PVA-SG hydrogel tailored with mechanical properties to selectively drive development of Schwann cells (SCs)

2

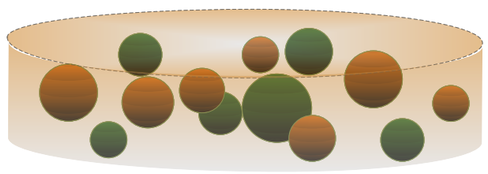

Legend

Glial progenitors

Neural progenitors

Degradable 10 wt% PVA-SG

Hypothesis: Hydrogel cell carrier that supports SCs development supports neuronal development when cultured in simultaneous encapsulation

3

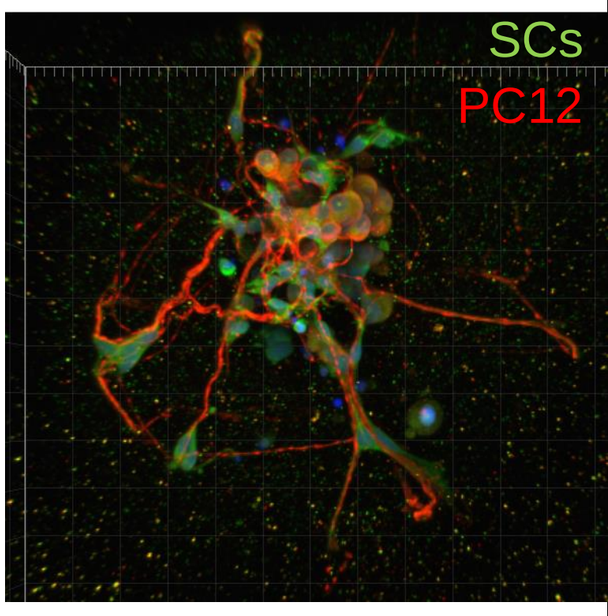

SCs and neuron-like PC12 cells in PVA-SG associating into a 3D neural network within 8 Days.

Cover Letter

To the Editors,

I am pleased to submit a paper entitled "Tissue engineered hydrogels supporting 3D neural networks" to Acta Biomaterialia Journal. The submission is a full paper detailing original research studies. All the authors have contributed to the research and preparation of the manuscript. This study is placed within the context of new material approaches for nerve tissue engineering and regeneration. This paper presents a systematic study that examines the role of hydrogel mechanics on glial cell morphology to ultimately promote neural-glia network formation. Previous research has shown that poly(vinyl alcohol) (PVA) based hydrogels with small amounts of protein content can be tailored to encapsulate cells in a 3D environment with mechanical properties resembling those from native nerve tissue. The major challenge addressed in this work was understanding the role of the dynamic degradable hydrogel cell carrier and the changing mechanical properties on both cell morphology and function. It assesses the hypothesis that a 3D environment tailored to support glial cell function will be well suited to supporting neuron growth when both cell types are co-encapsulated within the same hydrogel. It was shown that a hydrogel with an initially higher modulus, supports formation of more physiologically relevant Schwann cell morphologies and greater production of relevant ECM. Subsequently, these higher modulus hydrogels are shown to support development of neural networks with neural-glial cell interactions. These findings support the use of PVA hydrogels with tailored mechanics for delivery of cells for nerve tissue regeneration.

On behalf of the authors,

Regards,

Dr Ulises A. Aregueta Robles

Statement of significance

Hydrogels as platforms for tissue regeneration must provide encapsulated cellular progenitors with physical and biochemical cues for initial survival and to support ongoing tissue formation as the artificial network degrades. While most research focuses on tailoring scaffold properties to suit neurons, this work aims to support glia SCs as the key cellular component that physically and biochemically supports the neuronal network. The challenge is to modify hydrogel properties to support growth and development of multiple cell types into a neuronal network. Given SCs ability to respond to substrate mechanical properties, the significance of this work lies in understanding the relationship between dynamic hydrogel mechanical properties and glia SCs development as the element that enables formation of mature, differentiated neural networks.

Title Tissue engineered hydrogels supporting 3D neural networks

Ulises A Aregueta-Robles[1], Penny J Martens[1], Laura A Poole-Warren[1], and Rylie A Green[2]*

Dr. U. A. Aregueta-Robles, Prof. P. J. Martens, Prof. L. A. Poole-Warren and Dr. R. A. Green
1. Graduate School of Biomedical Engineering, University of New South Wales, Sydney, Australia.
2. Department of Bioengineering, Imperial College London, London, UK

Dr. U. A. Aregueta-Robles
E-mail:u.areguetarobles@unsw.edu.au

Keywords: biosynthetic hydrogel, tissue engineering, supporting glia, neural networks, polyvinyl alcohol.

Abstract

Promoting nerve regeneration requires engineering cellular carriers to physically and biochemically support neuronal growth into a long lasting functional tissue. This study systematically evaluated the capacity of a biosynthetic poly(vinyl alcohol) (PVA) hydrogel to support growth and differentiation of co-encapsulated neurons and glia. A significant challenge is to understand the role of the dynamic degradable hydrogel mechanical properties on expression of relevant cellular morphologies and function. It was hypothesised that a carrier with mechanical properties akin to neural tissue will provide glia with conditions to thrive, and that glia in turn will support neuronal survival and development. PVA co-polymerised with biological macromolecules sericin and gelatin (PVA-SG) and with tailored nerve tissue-like mechanical properties were used to encapsulate Schwann cells (SCs) alone and subsequently a co-culture of SCs and neural-like PC12s. SCs were encapsulated within two PVA-SG gel variants with initial compressive moduli of 16 kPa and 2 kPa, spanning a range of reported mechanical properties for neural tissues. Both hydrogels were shown to support cell viability and expression of extracellular matrix proteins, however, SCs grown within the PVA-SG with a higher initial modulus were observed to present with greater physiologically relevant morphologies and increased expression of extracellular matrix proteins. The higher modulus PVA-SG was subsequently shown to support development of neuronal networks when SCs were co-encapsulated with PC12s. The lower modulus hydrogel was unable to support

effective development of neural networks. This study demonstrates the critical link between hydrogel properties and glial cell phenotype on development of functional neural tissues.

1. Introduction

Neurological injuries and disorders represent a major public health problem affecting up to one billion people worldwide. With limited regenerative ability, nerve tissue requires assistive technologies to promote tissue healing and restoration of nerve function. Tissue engineering for nerve tissue regeneration has been approached by exploring the delivery of cellular progenitors within biomimetic scaffolds. Ideally, a neural scaffold should present cells with physical and chemical cues to induce expression of phenotypes resembling *in vivo* tissue. Hydrogels are polymer systems with physical and biochemical properties that can be tailored to present cells with a microenvironment that more closely resembles the extracellular niche [1-3]. However, control of the structure and mechanical properties of hydrogel networks largely depends on selection of fabrication technique and chemical composition [1, 2, 4]. This presents a key challenge for the development of hydrogel technologies that aim to allow controlled degradation to support timely neuronal development.

Although hydrogel degradation can be tailored, as the cellular scaffold degrades there is a loss in both mechanical integrity and physical cues. Without these cues, cells grown within 3D scaffolds lack organisation and the overall cell growth may not reflect the desired tissue structure or function [5]. While the neurons are critical to the function of nerve tissues, *in vivo* they are supported by accessory cells known as glia. These neuroglia are the cells that present trophic and physical support to the neurons both during *in utero* development and within the dynamic biological environment. However, simultaneously encapsulating glia and neuronal progenitors within a hydrogel also presents challenges. Conventional cultures use a layered or multistep process to

combine multiple cell types as they respond to different growth and differentiation cues. When using an encapsulation approach where all cells are incorporated within the hydrogel carrier during gelation, this is not possible. It is therefore proposed that for appropriate neuronal development, cellular scaffold properties should be modified to target not the neurons but the neuroglia. It was hypothesised that a hydrogel cell carrier tailored to selectively drive phenotypic development of neuroglia will consequently support the formation of a neuronal network during and following hydrogel degradation. The key challenge addressed in this work was to understand how modulation of degradable hydrogel mechanical properties affects the development of functional glial cell phenotypes to further enable formation of neuronal networks as the hydrogel carrier degrades.

Substrate mechanical properties play a key role in phenotypic modulation of both glial [6-10] and neural cell morphologies [11-14]. Neuroglia such as Schwann cells (SCs) develop bipolar processes that are ideal for supporting neurite development when cultured on 2D substrates with mechanical moduli ranging from 2 kPa to 5 kPa [9]. However, neurite outgrowth is enhanced when neural cells are grown on substrates an order of magnitude softer, ranging from 0.05 kPa to 0.275 kPa [11-14]. Although neurons are responsible for transmission of action potentials, the supporting neuroglial cells (such as SCs or astrocytes) [15] and associated extracellular matrix (ECM) are critical elements that support neural function. Glial cells and in particular SCs in the peripheral nervous system (PNS), provide neurons with topographical cues [16], production of ECM rich in growth and differentiation factors [17], as well as with homeostatic and synaptic support [15]. Therefore, to enable long-term maintenance and support of the neuronal network, it is essential to understand the role of hydrogel degradation and mechanics of glia development into a supporting matrix before degradation is complete.

While remarkable results have been shown when using hydrogel materials to support *in vitro* growth of neurons, most approaches use ECM rich systems [18-20] or biological materials [21-26], which do not allow for fine control of mechanical properties. Studies have also used hydrogels as

cellular carriers and assessed glial development as a part of a neuronal mixed culture, such as primary tissue explants [18, 20, 27] or stem cells [22-25, 28-30], however these studies do not allow decoupling of the effect of the 3D hydrogel mechanical environment from the presence of exogenous growth factors present in the ECM rich environment or produced by other cell types. In this study, a primarily synthetic hydrogel carrier with tailored mechanical properties was specifically assessed for support of neuroglial SCs with a focus on their capacity to express physiologically relevant morphologies and ECM.

Poly (vinyl alcohol) modified with tyramine (PVA-Tyr) residues has been shown to enable control of the polymer carrier mechanical properties while allowing incorporation of tyrosine rich biomolecules to support cellular interactions [31]. In particular, the PVA-Tyr system allows covalent crosslinking with unmodified sericin and gelatin (PVA-SG) to respectively protect cells from the initial polymerization process and present cells with initial attachment cues. Previous research by Aregueta-Robles *et al*. [32] has shown that PVA-SG can be tailored into polymeric scaffold variants that present SCs with a compressive modulus (K) from 2 kPa to 16 kPa, which is comparable to literature reports of nerve tissue stiffness [6, 33]. While it was demonstrated that SCs survived and remained viable following the initial polymerisation process, the cell growth and development into functional phenotypes was not examined. In this study, the capacity of PVA-SG hydrogels to support phenotypical SC morphologies and their consequent ability to support neuronal network growth was assessed.

SC and PC12 cell lines were selected as a neuronal co-culture model in preference to primary tissue explants used in prior studies [34]. The clonal cell system is highly reproducible and minimises the number of cellular components and growth factors which can incorporate confounding variables when assessing the effect of hydrogel mechanical properties on neuronal and glial development. The 3D co-culture of SC and PC12 cells developed in this study also established the translation of a 2D co-culture into a 3D system. It demonstrated a feasible approach for simultaneous seeding,

growth and differentiation of both cell types within the 3D hydrogel. These results offer unprecedented evidence of a highly repeatable cell encapsulation system consisting of neuron-like and glial cell lines growing and developing into neuronal networks when simultaneously encapsulated within a biosynthetic hydrogel. Of particular note was the differentiation and transition of PC12 cells into neuronal networks in response to the structural and biochemical support of SCs.

2. Materials and Methods

2.1 SC and PC12 culture

All chemical, reagents and proteins were purchased from Sigma-Aldrich unless otherwise stated. SCs (SCL4.1/F7, 93031204) were proliferated in media composed of Dulbecco's Modified Eagle's Medium (DMEM, D7777) supplemented with 10% fetal bovine serum and 1% penicillin/streptomycin (Gibco). Cellular incubation was performed at 37°C, 5% CO2, 100% humidity. Confluent monolayers were dissociated with Trypsin-EDTA (1X, 59430) for experiments and passages. Cells for experiments were in log phase with a passage number between 12 - 30. Pheochromocytoma cell line (PC12, 88022401) was maintained with proliferation media solution consisting of Roswell Park Memorial Institute medium (RPMI-1640) supplemented with 10% horse serum (HS), 5% FBS and 1% P/S. Cells for experiments were in log phase with a passage number between 10-20.

2.2 PVA-SG Hydrogel fabrication

Two variations of PVA-SG were fabricated via changes on macromer content as previously described [32]. In brief, gelatin (1 wt%) from porcine skin, (1 wt%) sericin bombix mori and PVA-Tyr (8 or 3 wt%) were dissolved one component at a time in DPBS at 80 °C. Tris(2,20-bipyridyl)dichlororuthenium(II) hexahydrate (Ru) and Sodium persulfate (SPS) were used as photoinitiators for polymerization. Ru and SPS concentration of 0.6 mM and 6 mM, respectively,

were used to produce 5 wt% PVA-SG hydrogels and 1.2 mM and 12 mM for 10 wt% PVA-SG. Upon complete dissolution, the solution was cooled to RT and photoinitiators were added.

2.3 Cellular encapsulation in PVA-Tyramine/Sericin/Gelatin (PVA-SG) hydrogels

Prior to polymerisation, 10^7 cells were added per mL of macromer solution and gently mixed by aspiration. The mixture was promptly poured into the silicone moulds (8 mm diameter, 0.5 mm thickness). Gelation was carried out by immediately irradiating the samples with visible light at 15 mW/cm^2 for 3 minutes. A total of 9 cell laden hydrogels for each sample set (3 repeats with 3 replicates, n=3) were immediately placed into tissue culture dishes for incubation with complete media for 3 days and then fed with low serum media for 7 days. This culture media strategy was proposed to allow neuronal differentiation conditions while providing a temporary recovery and support for all cells following encapsulation. A control group of SC only hydrogels was cultured with high serum media only to assess viability and proliferation effects related to serum reduced in media. Co-encapsulation of SC and PC12 cells was performed at 10^7 cells were added per mL of macromer solution with a proposed 9:1 SC: PC12 cells ratio. Co-cultures were supplemented with NGF (50ng/mL, 2.5S, Jomar Bioscience) upon media shift to low serum conditions. A control group of encapsulated standalone PC12 cells was included to assess the supporting effect of SCs to promote neurite outgrowth.

2.4 Compressive modulus of PVA-SG hydrogels

To examine the impact of cells on hydrogel mechanics, compression testing was performed. Hydrogels with and without cells were assessed by uniaxial compression testing using an Instron 5543P3124 mechanical tester. A 50N load cell was applied at a crosshead speed of 0.5 mm/min. The compressive modulus was calculated as the slope of stress vs strain given by the relation $Y=(F/A)/(\Delta L/L)$, within 5 % - 15 % strain. Compressive tests were performed at 2, 5 and 10 days.

2.5 Live-dead assay

To assess viability of encapsulated cells a fluorescent live/dead assay (Calcein-AM/propidium iodide) was used. Samples were incubated for 10 mins with 1µM calcein-AM and propidium Iodide (1 µg/mL in DPBS). Samples were rinsed three times with DPBS and then analysed using an epifluorescent microscope (Zeiss, Axioshop 2 MAT). Green fluorescent cells were regarded as alive, red fluorescent cells were considered as dead cells. Cellular viability was calculated as the percentage of living cells to the total number of cells (live + dead).

2.6 Cellular proliferation

To determine the number of metabolically active cells within the hydrogel, a fluorescent assay based on the ability of viable cells to reduce an indicator dye (resazurin, CellTiter blue, promega, G8080) was used. Resazurin becomes fluorescent (resorufin) in the presence of metabolically active cells. Cell laden hydrogels were incubated for 3 hours with resazurin at a working concentration of 0.2 mg/mL. 100 µL of supernatant was transferred to an opaque 96-well plate for florescence recording (544nm/590-10nm, Ex/Em). A control without cells was included to subtract background fluorescence of media. In parallel for each repeat, SCs were plated in a 12-well plate as a control to estimate the number of metabolically active cells. SCs were seeded at densities ranging from $10x10^3$ to $300x10^3$ cells per well. After 24 hours cells were incubated for 3 hours with resazurin. Media was recovered and transferred to an opaque 96 well plate for fluorescence reading as stated above. To determine the total number of cells per gel, cell nuclei were stained with bisbenzimide. Samples were fixed with 4% formaldehyde overnight at 4°C and then washed three times with DPBS (10 mins incubation between washes) and then blocked with a solution of 2% bovine serum albumin, 0.1% Triton X-100 and 0.2% gelatin in DPBS for 30 mins. After blocking, samples were permeabilised with a 0.5% Triton X-100 solution in DPBS for 30 mins and samples were counterstained with bisbenzimide (Hoechst 33342, 1:10000, Molecular Probes).

2.7 Morphological analysis of SCs

To assess SCs morphology cell laden hydrogels were immunostained with anti-S100, a protein abundantly expressed in mature Schwann cells [17]. Samples were fixed, blocked and permeabilised as described in section 2.6. Cells in gels were directly immunostained with anti-S100 (rabbit polyclonal; Z0311; 1:40; Dako, Agilent Technologies). FITC (IgG anti-rabbit; 4030-02; 1:200; Southern Biotechnology) was used as secondary fluorophore-conjugated antibody. Bisbenzimide (Hoechst 33342, Molecular Probes) was used for nuclei staining. Cells were observed using confocal laser-scanning microscopy (Olympus, FluoView 1200). All cell imaging in this work was performed using a confocal laser-scanning microscope (Olympus, FluoView 1200) through a 40x 0.7 oil immersion objective. For each hydrogel composition and for each time point, a total of 9 hydrogel discs were fabricated (3 repeats, 3 replicates each repeat, n = 3). Z-stack images were processed in Imaris® software to render a 3-D construct of encapsulated cells. Cells imaged in the Z-stack were individually analysed and classified according to the number of outgrowing cytoplasmic processes as well as their resemblance to physiologically relevant. A cell was considered to have developed a cytoplasmic process whenever the extension was longer than that of a single cell body (soma). Cells with processes shorter than the soma were classified as pseudopodia. Cells with one or two processes shorter than the soma were regarded as oval cells. Cells were classified as bipolar whenever one or two cytoplasmic processes extended away from the soma in a straight line (at 180° to each other). Cells outgrowing processes in non-straight lines, at varied angles were classified as having “Extended processes” but not specifically exhibiting bipolar morphology. Groups of cells forming linear arrangements were regarded as “cells in bands”. Cells presenting with only pseudopodia or having oval shapes were merged in one group. Cells without processes that adopted a spherical shape were classified as “non-polar” and a last group of cells, which showed nuclear fragmentation, was included. The occurrence of a particular morphology was reported as the percentage of a given classification with respect to the total cell count.

2.8 Extracellular matrix production and neurite outgrowth

Semi quantitative analysis of laminin, collagen-IV and βIII-tubulin expression was performed by recording the fluorescence intensity using a confocal microscope. Encapsulated SCs were immunostained for detection of laminin and collagen-IV and βIII-tubulin for co-cultures. Samples were fixed and blocked as described in section 2.6. To assess the expression of both proteins outside cell bodies, cells in gels were not permeabilised and directly immunostained with anti-laminin (chicken polyclonal; ab14055; 1:200; abcam), anti-collagen-IV (rabbit polyclonal; ab6586; 1:50; abcam) and anti-βIII-tubulin (mouse polyclonal; ab78078; 1:200; abcam). Secondary fluorophore-conjugated antibodies were used, being FITC (IgG anti-rabbit; 4030-02; 1:200; Southern Biotechnology), Alexa Fluor 555 (IgG anti-chicken; A-21437; 1:200; Life technologies), for collagen IV and laminin respectively and (IgG anti-mouse; PIE35513; 1:200; Thermo Fisher) for βIII-tubulin. For nuclei staining cells were permeabilised and the counterstained with bisbenzimide. Cells were observed using confocal laser-scanning microscopy (Olympus, FluoView 1200). Laminin and collagen-IV production was assessed immediately after polymerisation to establish a baseline and compared to constructs as the cells developed at day 2, 5 and 10. In brief, confocal z-stacks used for image analysis were taken with a 1024x1024x20 (X, Y, Z) number of voxels with a voxel size of (0.31, 0.31, 0.41 μm). No brightness or contrast adjustments were made on processed images. An initial background fluorescence subtraction was performed through Gaussian filter included in Imaris image processing options. Then a mask was created on voxels associated with laminin or collagen absolute fluorescence without any threshold adjustments. A final surface was rendered, which was used to retrieve volume of containing voxels. The total volume of either laminin or collagen-IV per time point was normalised to the number of cells.

2.9 Neurite outgrowth of PC12 cells

To assess the degree of neurite outgrowth in PC12 cells, volumetric changes associated with neurite outgrowth were measured through expression of βIII-tubulin using confocal microscopy as

described in section 2.8. To compare supporting potential of SCs in 3D, an additional sample group of PC12 only cells were encapsulated at the same cellular seeding density for PC12 cells in co-culture ($1x10^6$ cells/mL). The amount of βIII-tubulin associated with neurites per PC12 cell was analysed at 2, 5 and 8 days and presented as normalised β-III tubulin volume (μm^3/cell). The analysis of neurite outgrowth based on βIII-tubulin volume rendered from confocal z-stacks was validated in 2D cultures as described in supplementary data.

2.10 Statistical analysis

All reported values represent the mean of 3 repeats (n=3), each repeat consisted of 3 replicates, N=9. One-way ANOVA was performed to compare means of groups. Tukey-Kramer test was used for multiple comparisons between means. Means of groups were considered different at a significance level of 5% ($p < 0.05$). Normal distribution of residuals was confirmed by means of a chi-square goodness-of-fit test.

3. Results

3.1 Survival and metabolic activity of encapsulated Schwann cells

The average cell viability of SCs within PVA-SG is shown in Figure 1A for both high and low serum conditions. At Day 2, when both sample sets were supported with high serum, cellular viability was close to 90% in both 5 and 10 wt% gels. Cells in the 10 wt% hydrogels did have slightly lower viability, which was expected to be a result of the higher concentration of the initiator, SPS, required for the polymerisation of this hydrogel. This initiator creates sulphate radicals that are known to impact on cellular viability [35]. Despite reducing serum content in media (from 10% to 1%), close to 60% of the SC population remained viable across the study period.

Figure 1B shows the ratio of SCs within the encapsulated population presenting with metabolic activity. The activity levels of the cells varied throughout the 10 day experiments, and the %

macromer was shown to influence this activity differently across the time points. At Day 2, SCs in 10 wt% gels were more metabolically active (53% vs 39%). By day 5, cells in 10 wt% gels were less active (60% vs 80%). It was found that metabolic activity of cells cultured in a reduced serum media was ~1.5 times higher than cells in high serum media. Finally, at Day 10, the metabolic activity of cells cultured in 10 wt% PVA-SG was 2.4 times higher in a reduced serum media than in high serum media. At this time point the cellular population of 5 wt% hydrogels could not be determined as a result of the dispersal of these degradable samples in the solution, preventing accurate analysis of the fluorescent signal. Based on this limitation an additional time point at 8 days (Day 8) was included for cellular morphology and ECM studies.

3.2 Impact of hydrogel scaffold mechanics on cell morphology and function

The initial K for 10 wt% and 5 wt% PVA-SG hydrogels was 16 ± 3.4 kPa and 2.3 ± 0.4 kPa, respectively. As shown in Figure 1C, consistent with a prior study [36], the compressive modulus of the hydrogel significantly decreased in both systems due to incorporation of cells. As suggested by Bryant *et al*. [36] cells as deformable objects could be buffering the hydrogel compressibility, a phenomenon expected to be more notable for low moduli systems. Despite of the decrease in K, 10 wt% PVA-SG hydrogels presented cells with a K ranging from 1 kPa - 2 kPa from Day 1 to Day 5 before decreasing to 0.5 kPa. Comparable studies have shown that this range of mechanical moduli promotes glial differentiation into supporting phenotypes [37]. In contrast, the K of cell laden 5 wt% PVA-SG was lower than 1 kPa by Day 2.

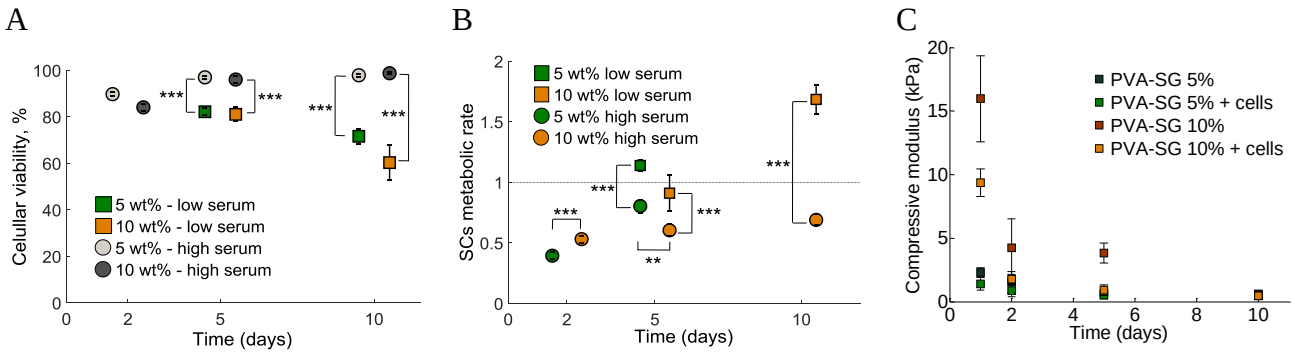

Figure 1. (A) Viability of SCs embedded in 5 wt% (green) or 10 wt% (orange) hydrogels. (B) Metabolic activity of SCs encapsulated in 5 wt% (green) and 10 wt% (orange) PVA-SG hydrogels. Dispersal of 5 wt% hydrogel samples at limited analysis of fluorescent signal at Day 10. Cells cultured with differentiation media (square) compared to cells in proliferation media (circles) from Aregueta-Robles *et al*. [32] (C), K of 5 wt% and 10 wt% hydrogels with or without cells. Error bars are 1 SD, (*** $p<0.001$).

Representative images of SCs grown in PVA-SG hydrogels are depicted in Figure 2. It was shown that by Day 2 cells have established cell-cell associations, adopted active morphologies and extended cytoplasmic processes in multiple directions. Figure 3 shows the percentage of SCs extending cytoplasmic processes. At Day 2 and Day 5, SCs extended a greater number of processes within 10 wt% hydrogels than 5 wt% hydrogels as shown in Figure 3A and 3B. At these points the 10 wt% hydrogel's K ranged between 1 kPa – 2 kPa. In contrast, about 80% of SCs encapsulated within 5 wt% hydrogels remained in a spherical shape (80%), which were presented with a K lower than 1 kPa by Day 2. As both the 5 and 10 wt% hydrogels continued to degrade there was a decrease in the occurrence of cytoplasmic extensions and length of processes. At 8 days, the number of cells with only pseudopodia extensions was dominant in both systems. No differences were observed in the percentage of processes between 5 wt% and 10 wt% hydrogels at this time (Figure 3C). By Day 10, approximately half of the cell population in 10 wt% PVA-SG had developed one or two cytoplasmic processes and about 25% of cells extended pseudopodia (Figure 3D).

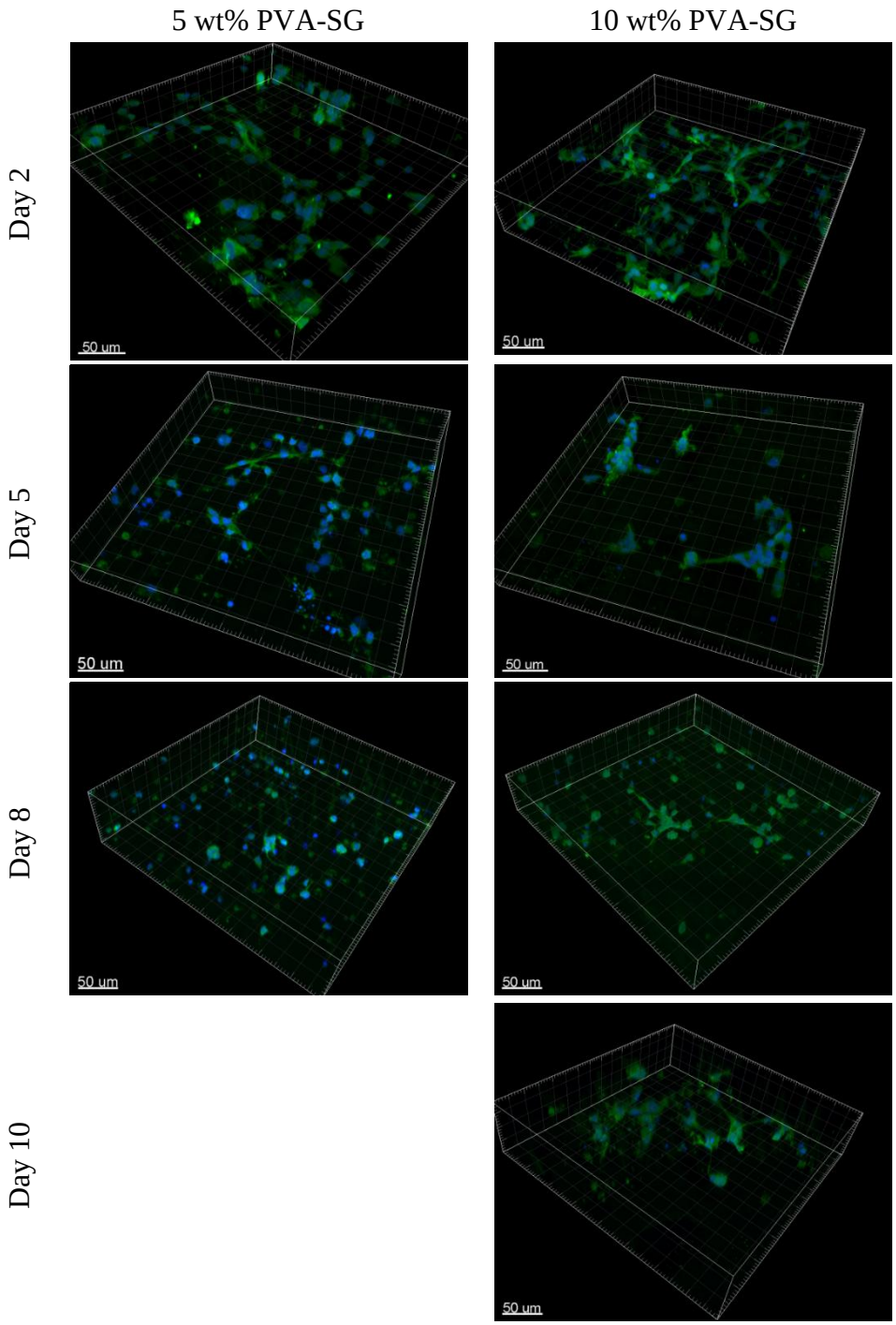

Figure 2. Three dimensional distribution of SCs in PVA-SG hydrogels. Confocal Z-stacks of S100 (green) and nuclei (blue) were constructed using Imaris software.

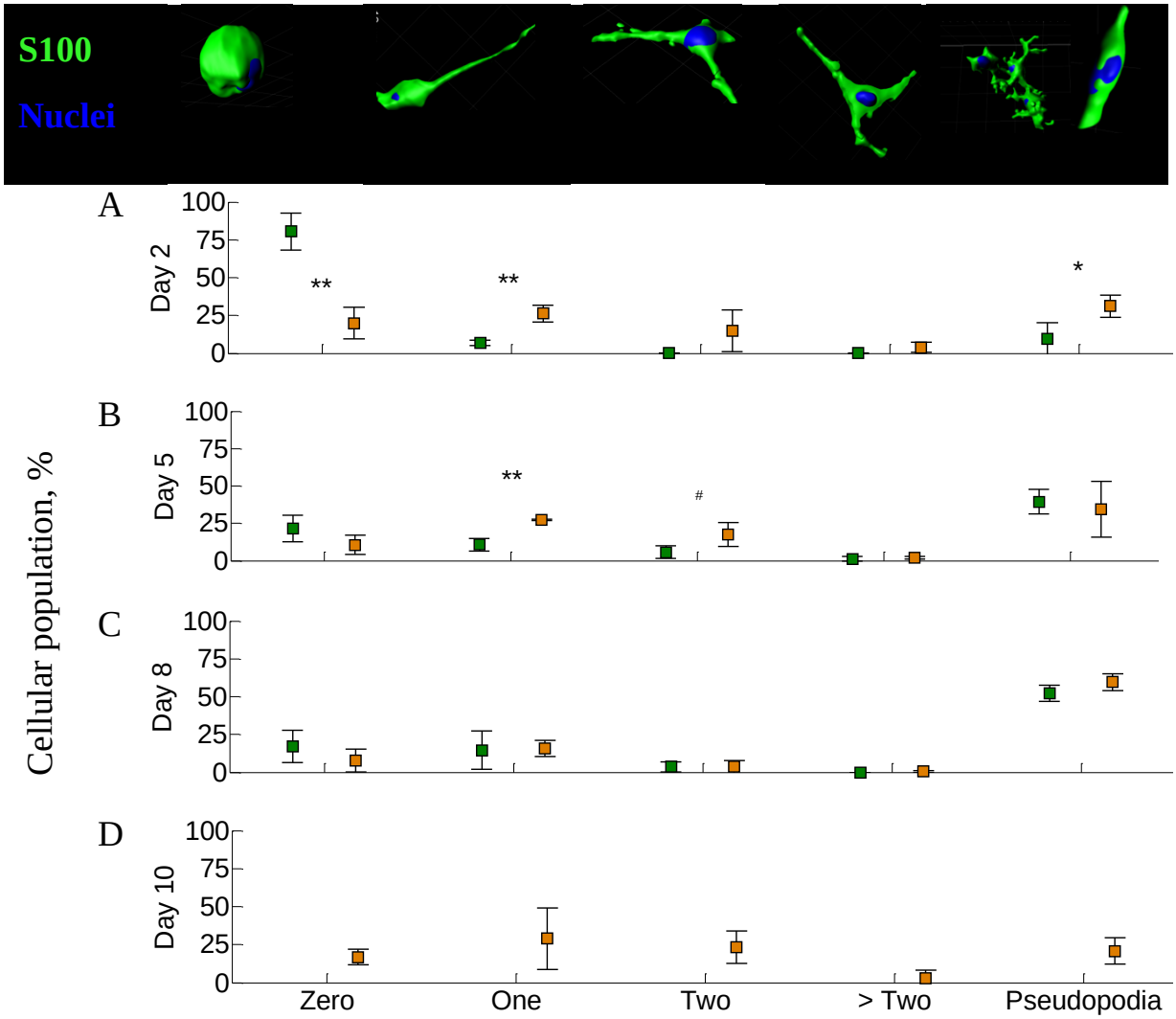

Figure 3. SC extension of cytoplasmic processes in 5 and 10 wt% PVA-SG at 2, 5, 8 and 10 days post encapsulation. Top, confocal images used to generate a surface rendered 3D image of cells at various morphologies. Cells encapsulated in 5 wt% (green) or 10 wt% (orange). 5 wt% hydrogels at Day 10 were unable to be processed due to hydrogel disintegration during immunostaining processes. Error bars are 1SD, (n=3), (*** $p<0.001$, ** $p<0.01$, * $0.01<p<0.05$).

Figure 4 depicts the expression of cellular structures related with physiologically relevant morphologies. These structures identified as bipolar, linear arrangements of cells (cells in bands), pseudopodia and oval shaped cells, hold a physiological relevance during the development of PNS [17]. At Day 2 post-encapsulation, about 12% and 18% of SCs cultured within 10 wt% PVA-SG were adopting bipolar morphologies and arranging in cell bands, respectively. This expression was significantly higher than cells in 5 wt% gels, where less than 1 % of cell population expressed these morphologies. More frequently SCs extended cytoplasmic processes without a bipolar arrangement

(~25%) or presented with either pseudopodia or an oval shaped structure (~25%). The occurrence of these cellular structures was maintained by Day 5 and remained significantly higher in 10 wt% than in 5 wt% gels. At Day 8, no differences were observed in cell numbers adopting phenotypical morphologies between the 5 wt% and 10 wt% PVA-SG gels. At this stage, cells extending pseudopodia were dominant in both systems (Figure 4C). By 10 days post-encapsulation, approximately 50% of cells in 10 wt% PVA-SG gels retained bipolar morphologies or were associating into linear arrangements. About 25% of cell population had developed one or two cytoplasmic processes and the rest of cells had extended pseudopodia (Figure 4D).

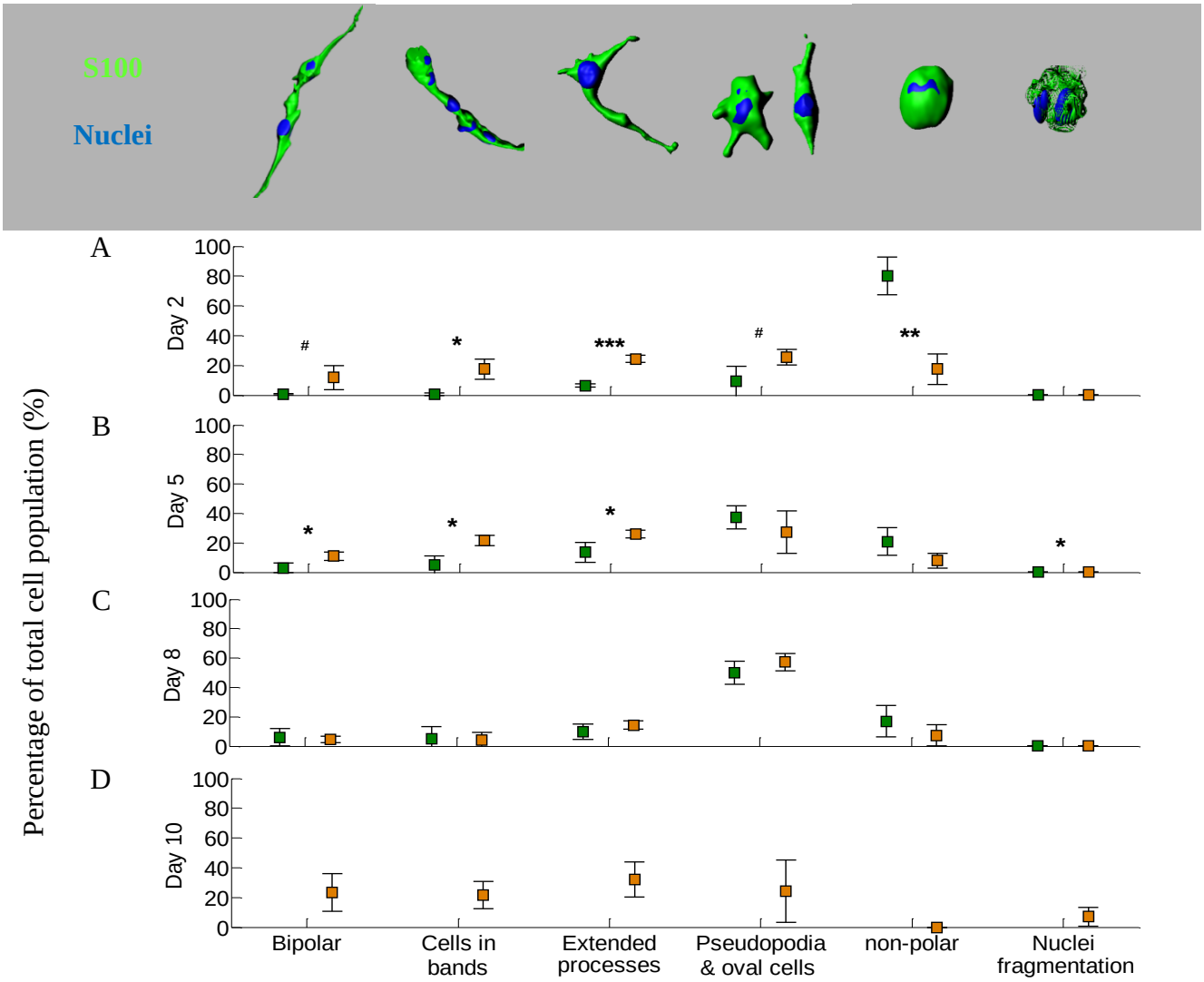

Figure 4. Morphological presentation of SCs in 5 wt% and 10 wt% PVA-SG at 2, 5, 8 and 10 days post-encapsulation. Top, surface rendered 3D image of cell morphologies. Cells encapsulated in 5 wt% (green) or 10 wt% (orange). 5 wt% hydrogels at Day 10 were unable to be processed due to hydrogel disintegration during immunostaining processes. Error bars are 1SD, (n=3) (** $p<0.01$, * $0.01<p<0.05$, # $0.05<p<0.1$).

3.3 **ECM production during hydrogel degradation**

Representative images of laminin and collagen production by the SCs are shown in Figure 5. Both laminin (red) and collagen-IV (green) were expressed on the outer surface of the SC membranes at all time points and in both hydrogel compositions. As shown in Figure 6A, expression of laminin per cell significantly increased about 5 times over the first 5 days in both 5 wt% and 10 wt% hydrogels ($p <0.001$), respectively. This degree of laminin expression was maintained at Day 8 and Day 10 when 10 wt% hydrogels were close to the point of reverse gelation but not in 5 wt% hydrogels. Expression of Collagen-IV significantly increased from Day 0 to Day 5 about 4 and 5 times in 5 wt% and 10 wt% gels, respectively (Figure 6B). In contrast to laminin, Collagen-IV expression significantly decreased from Day 5 to Day 8. In both gel systems the highest expression of collagen-IV and laminin occurred when the compressive modulus hydrogels ranged around 1 kPa (Figure 6C and 6D). However, collagen expression dropped to baseline levels when gels where at the lowest K, close to the point of complete degradation.

No significant differences were observed between 5 wt% and 10 wt% hydrogels. However, there were differences of cellular distribution as well as in volumetric changes between hydrogel compositions due to swelling that could be masking changes in ECM molecules expression. A higher and more variable cellular density was observed in 5 wt% gels than in 10 wt% gels. Consistent with previous reports, the lower macromer concentration resulted in hydrogels that experienced a decrease in volume of 10-30% following polymerisation [32]. In addition, it is possible that the 5 wt% hydrogel solution, which results in a less viscous solution, is allowing cells to settle before polymerisation. Moreover, hydrogels at 10 wt% presented an increase in volume of 1.24, 1.75 and 1.74 times more than 5wt% at Day 2, 5 and 8, respectively. This difference indicates

that the microenvironment in 10 wt% hydrogels is expanding 24% to 70% more than in 5wt% hydrogels. Therefore, the amount of protein expressed by cells in 10 wt% hydrogels represents a lower volume fraction when compared to 5wt%. Taking these volumetric and cellular density changes into consideration it can be estimated that cells in 10 wt% hydrogels produced 2.2 ($p<0.001$) and 1.7 ($0.1>p>0.05$) times more laminin and collagen than cells in 5 wt% gels, respectively.

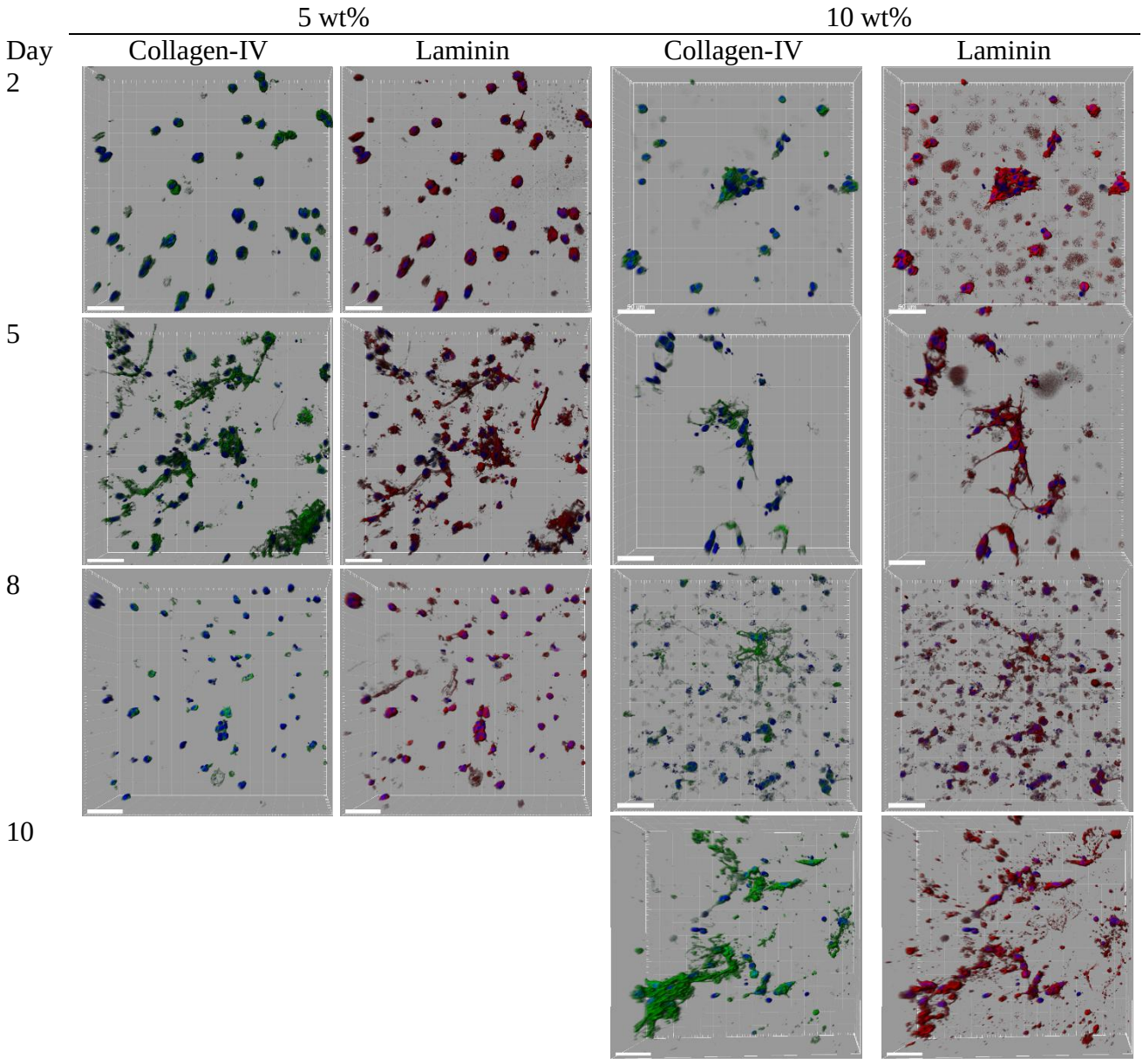

Figure 5 SCs expression of collagen-IV (green) and laminin (red) in 5 wt% and 10 wt%. Scale bars = 50 µm. Confocal Z-stacks were constructed using Imaris software.

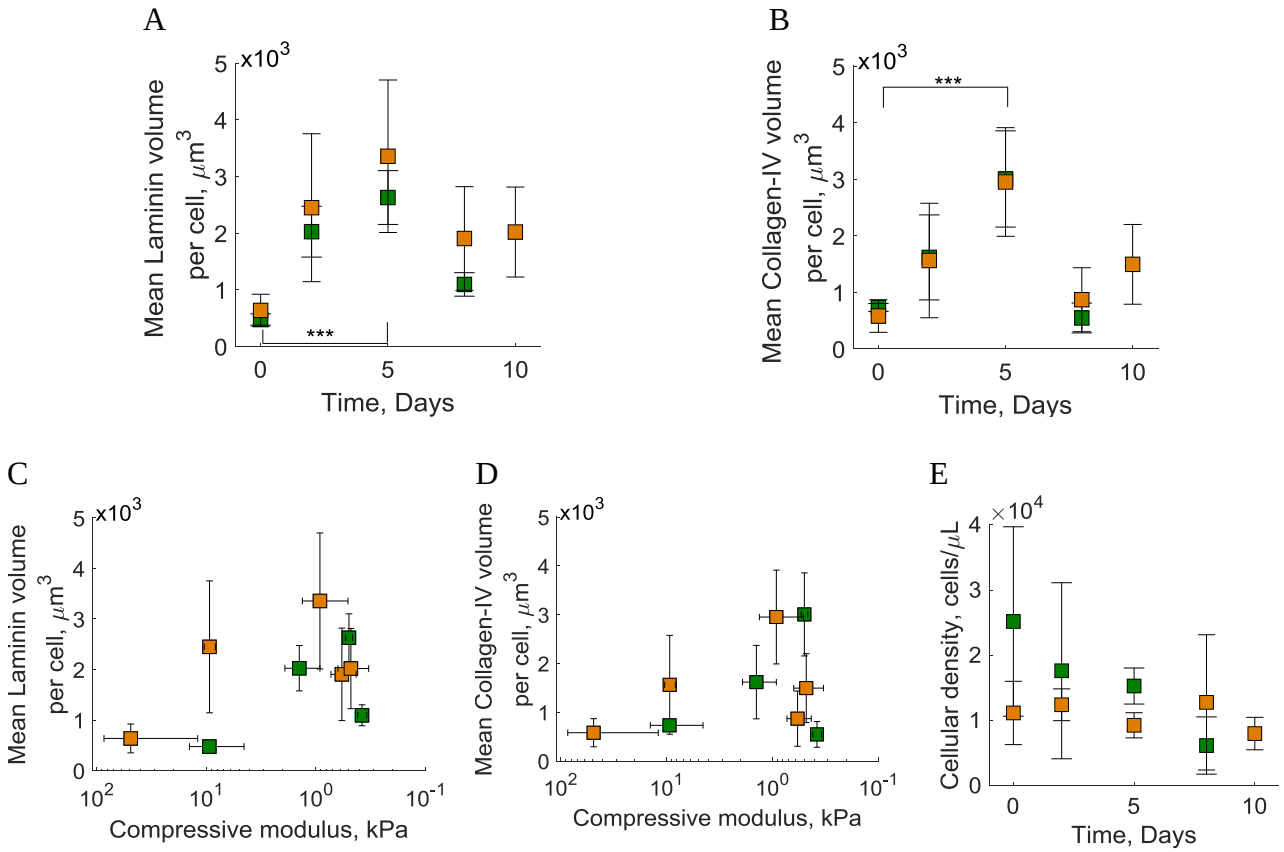

Figure 6 Semi-quantitative analysis of laminin and collagen-IV production as function of time (A and B). Cells encapsulated in 5 wt% (green square) or 10 wt% (orange square). Expression of laminin and collagen-IV as function of compressive modulus (C and D). The volume per cell was calculated from rendered surfaces using Imaris software. (E) SC density in 5 wt% or 10 wt%. Error bars are 1SD (*** $p<0.001$, n=3). 5 wt% hydrogels at Day 10 were unable to be processed due to hydrogel disintegration during immunostaining processes.

3.4 Survival and metabolic activity of SCs and PC12s co-encapsulated in PVA-SG

The average cellular viability and metabolic activity of SCs co-encapsulated with PC12s is shown in Figure 7A. Simultaneously encapsulated SCs and PC12 remained highly viable across the study period, with the lowest viability of ~75% by Day 8. Similar to viability, co-cultured cells presented with increasing metabolic activity over the 8 day study period. Figure 7A shows resorufin fluorescence associated with cellular metabolic activity of encapsulated SC/PC12 cells. At Day 2, encapsulated SC/PC12 cells presented a lower metabolic activity when cultured in high serum media. This impact on metabolic activity was also found in standalone encapsulated SCs. Following serum reduction and supplementation of nerve growth factor (NGF), metabolic activity significantly increased at Day 5 (2.1 fold) and was observed to be highest at Day 8 (2.7 fold). In addition, SC

population increased about 70% in co-culture with PC12 cells (Figure 7B), in contrast with standalone encapsulated SC which decreased 20% from Day 2 to Day 5.

As shown in Figure 7C, PC12 cells in simultaneous encapsulation with SCs presented a neurite outgrowth of about 4 times higher ($p<.001$) than PC12 only cultures from Day 5 onwards. Although PC12 cells as standalone or in co-encapsulation with SCs were being supplemented with NGF, the significant increase in neurite outgrowth is a clear indication of supporting effect of SCs.

3.5 SC support of PC12 cells related to morphological characteristics

Encapsulated SCs were found either in association with PC12 cells, as groups of SCs or as single cells (Figure 7D). As the hydrogel degrades and upon culturing cells with differentiation media, PC12 cells grew extensive neurites and associated with SC bodies adopting structures classified as clusters and cellular networks. Z-stacks of encapsulated SCs and PC12 cells at each time point are shown in Videos 1-3. Video 4 illustrates instances where PC12 cells and SCs were organising into either clusters or networks. While PVA-SG hydrogel (10 wt%) was able to support extensive neurite outgrowth of standalone encapsulated PC12 cells (Figure 7E and 7F), SCs were found to structurally support PC12 cells into a more organized cellular network as shown in Figure 7F and 7G and in better detail in Video 3. Moreover, it was observed that neuronal networks developed having 5-12 SC per each PC12, whereas cell clusters presented less than 5 SC per PC12 (See Figure S-4). This indicates the potential of using glia:neuron ratio as a modulating factor to influence the formation of neuronal networks.

Imaging cell cultures at a lower magnification revealed that cell networks were associated with adjacent networks or clusters forming larger networks across the scaffold (Figure 7H). These bridged networks were supported by SCs bodies, which were co-localized with PC12 somas and outgrowing processes as well as with bridging neurites (see Video 5). Similar to 2D cultures, these results show that the 2D culture strategy can be translated into a 3D environment resulting in PC12

cells outgrowing intricate neurite networks decorated by laminin and collagen deposited by SCs (Figure 7I and 7J).

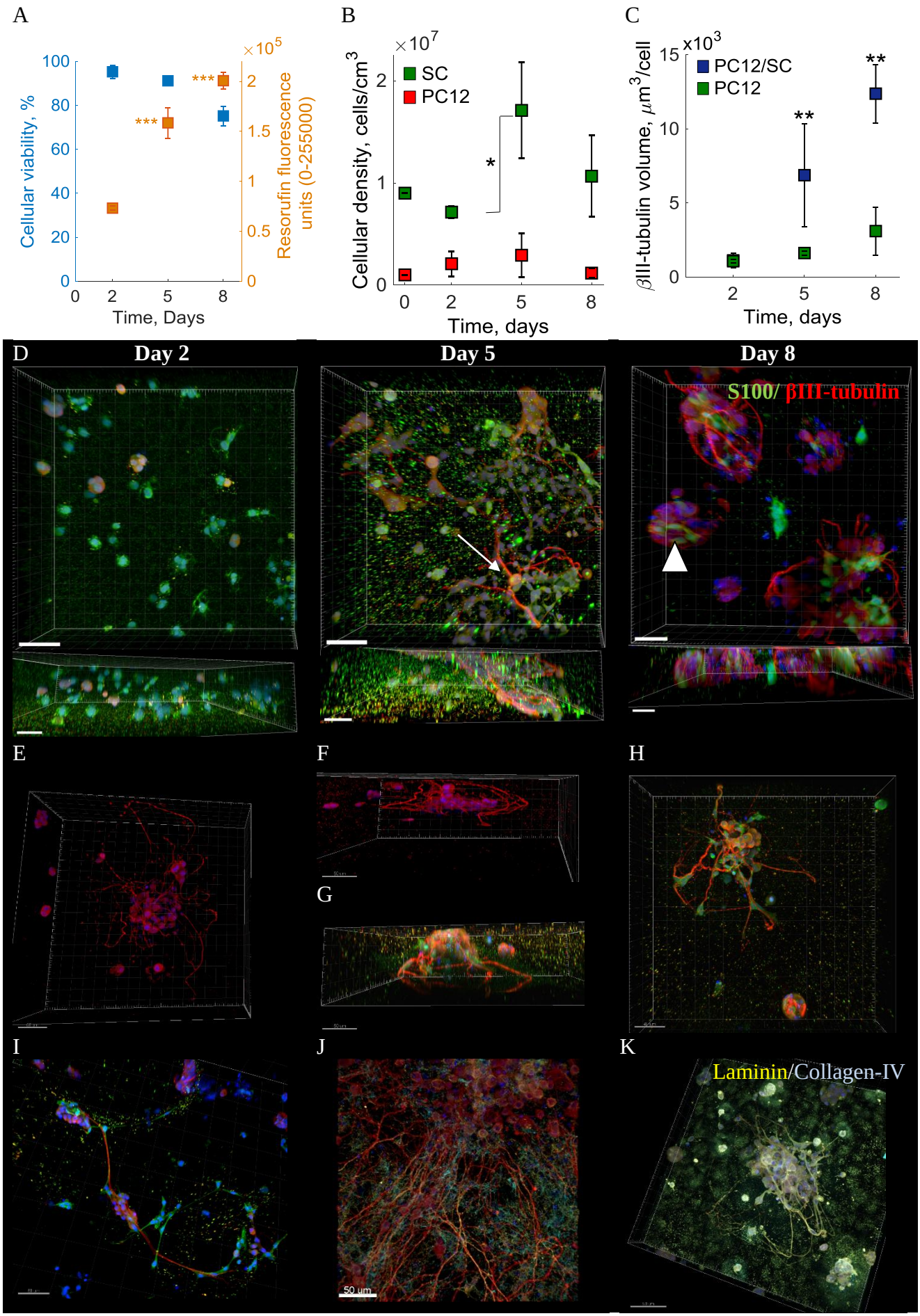
A
Cellular viability, %
Resorufin fluorescence units (0-255000)
Time, Days
B
Cellular density, cells/cm3
SC
PC12
Time, days
C
βIII-tubulin volume, μm3/cell
PC12/SC
PC12
Time, days
D
Day 2
Day 5
Day 8
S100/ βIII-tubulin
E
F
G
H
I
J
K
Laminin/Collagen-IV
50 um

Figure 7. (A) Cellular viability (blue) and metabolic activity (orange) of SC/PC12 encapsulated within 10 wt% PVA-SG. (B) Cellular density of SCs(green) and PC12 cells(red) in co-encapsulation within 10 wt% PVA-SG. (C) β-III tubulin volume expressed by encapsulated standalone PC12 cells (green) compared to PC12 cells in simultaneous encapsulation with SCs (blue). Error bars are 1SD, $p<0.0001$(***), $p<0.001$(**), $p<0.01$(*). (D) Top view (top) and side view (bottom) of encapsulated SCs and PC12 at Day 2, Day 5 and Day 8 assembling into co-culture networks (arrow head) or co-culture clusters (Arrow). Neurite outgrowth of standalone PC12 cultures in 10 wt% PVA-SG top view (E) and side view (F), compared to PC12 cells in co-culture with SCs side view (G) and top view (H). Cell networks in association with adjacent networks or clusters (I). Confocal Z-stacks of S100 (green), βIII-tubulin (red) and nuclei (blue) were constructed using Imaris software. Laminin (orange) and collagen-IV (cyan) deposited by SC on outgrowing neurites (red) in 2D (J) and 3D (K) co-cultures. Scale bars = 50 μm.

Overall the environment provided by the 10% PVA-SG hydrogel cell carrier allowed not only for cell survival and growth but for mutually supportive cellular interactions. This resulted in SCs and PC12 cells associating into neuronal networks expanding across the hydrogel as the scaffold degraded. These results offer unprecedented evidence of neuron and glial cell lines growing and developing into neuronal networks when simultaneously encapsulated within a biosynthetic hydrogel.

4. Discussion

Delivering neuronal progenitors within biomimetic scaffolds is a potential approach to support nerve regeneration. While hydrogel cell carriers can be tailored to degrade in a time frame consistent with the cellular ability to expand a cellular matrix, it is desired to enable the development of neuroglia as the key cellular component that physically and biochemically supports the neuronal network. However, this holds a significant challenge when growing simultaneously encapsulated mixed cell types with different growth and differentiation cues. The aim of the present work was to understand the relationship between modulation of hydrogel mechanical properties and SC development into functional phenotypes. This was assessed by measuring the capacity of SCs to adopt physiologically relevant morphologies, to express ECM molecules and to support growth of a neuronal network in response to the dynamic mechanics of degradable PVA-SG hydrogels.

SCs were shown to survive, grow and adopt physiologically relevant morphologies following encapsulation in PVA-SG degradable hydrogels with polymer content of 5 wt% and 10 wt%. These gels presented with an initial modulus of 2 and 16 kPa, respectively. It was found that high cellular viability and metabolic activity was supported by both 5 wt% and 10 wt% hydrogels over the 10 day study period. Extension of cytoplasmic processes and presence of elongated morphological characteristics were more prolific in the 10 wt% PVA-SG. The analysis on ECM production indicated that SCs expressed similar levels of ECM proteins in both hydrogel systems. However, hydrogel matrix expansion upon degradation in 10 wt% gels could be masking the overall protein expression. These results indicate that SCs survive within the hydrogel scaffold, but dynamically respond both morphologically and metabolically to their environment. Simultaneously encapsulated SCs and PC12s within the 10 wt% PVA-SG hydrogel presented with high viability and were shown to differentiate into their respective supporting glial and functional neuron-like phenotypes. Co-cultured SC and PC12 cells associated and organised into neuronal networks, both within localised areas and more extensively across the hydrogel construct.

Previous research has shown that SCs remain viable in both PVA-SG hydrogel variants when cultured in high serum conditions [32]. However low serum conditions are required when SCs are co-cultured with PC12s, to support neural cell differentiation [38-40]. As such, following 72 hours of support with high serum, one sample set was switched to low serum conditions. A trend of decreasing cellular viability with an increase in metabolic activity was found when encapsulated SCs were shifted to a low serum media required to support neuronal differentiation. This trend was not observed in cells cultured in a high serum media. This impact on cell survival has been observed by Syroid *et al.* [41] who reported that cellular metabolism of SCs increases as cellular viability decreases in response to low serum media. The opposite trend was observed when cells were treated with a high serum media remain viable but quiescent [41]. It is possible that the SC increase in metabolism is a response to serum deprivation in an effort to reach a neurotrophic source. While low serum provides the conditions in which neuronal differentiation is elicited due to removal of

mitogenic factors [39, 42], programmed cell death has been reported as a mechanism to adjust cell numbers, where cells that fail to secure a source of survival factors eventually die [42]. SCs are provided with survival factors upon close association with axons [43, 44]. Likewise, during this process SCs express ECM molecules that present neurons with attachment cues and growth factors [45, 46]. Cell viability was not detrimentally affected by the microenvironment provided by PVA-SG hydrogels, however the decrease in serum required to support neuronal differentiation, did reduce viability. It is possible that in the presence of neurons this effect may be lessened as SCs receive cues from the differentiating neural cells. Nonetheless, further research is required to elucidate the effect of a more representative *in vivo* environment where serum levels are not relevant and nutrients are mainly provided by extracellular fluid.

Maturation of nerve structures in peripheral nervous system depends in part on the ability for SCs to extend cytoplasmic processes. These cellular extensions are critical for SC migration, nerve fibre segregation and myelination [17, 47, 48]. It has been suggested in previous studies that glial cells develop more cytoplasmic processes when grown within scaffolds with mechanical modulus around 1 kPa to 2 kPa [37]. These results indicate that the 5 wt% PVA-SG (with approximately 10 times lower K), did not provide sufficient support for the SCs to anchor and grow cytoplasmic extensions. This conclusion is supported by studies undertaken by Zhou *et al.* [7] where it was demonstrated that SCs develop less processes when substrate stiffness is reduced below 0.76 kPa. Since hydrogels get softer as they degrade it is possible that cell adhesion sites are lost during this process. Gu *et al.* [10], conducted a study where SCs expressed lower amounts of cell-adhesion proteins as substrate stiffness decreased. Since SCs respond dynamically to substrate stiffness [7, 9, 10], it is possible that the softer material hindered the cellular capacity to extend processes. Alternatively, gelatin elution due to backbone degradation may further hinder cellular expansion.

Notably, it was observed that SCs cultured in 10 wt% PVA-SG more frequently adopted morphologies that resemble structures reported *in vivo,* than their 5 wt% counterparts. SCs can

dedifferentiate, resume proliferation and adopt morphologies to support tissue regeneration following nerve injury [17, 47]. Bipolar morphologies and linear arrangements of cell strands termed “Bands of Büngner” are common supporting morphologies, which provide regenerating axons with topographical and biochemical cues [17]. In addition, oval shaped cells with active pseudopodia hold a physiological relevance during the development of PNS [17]. The cellular population adopting bipolar morphologies or associating into cell strands was ~25 times higher when grown within 10 wt% than in 5 wt% hydrogels. This impact on phenotypic morphologies was mainly observed at Day 2 (Figure 4A) and Day 5 (Figure 4B) when hydrogel K was 1.7 kPa and 0.9 kPa, respectively. While mechanical modulus was similar to reported nerve tissue elastic modulus (0.2 kPa - 2kPa) [6, 33], this cellular response to hydrogel stiffness was minimal within 5 wt% PVA-SG which presented cells with a stiffness within 0.5 kPa - 1kPa during initial time points. It has been suggested that glial cells are better supported within the stiffer range of nerve tissue elastic modulus (1 kPa - 2 kPa) [7, 37]. Georges *et al.* [37] showed that astrocytes attach and adhere better when grown on ~1 kPa substrates based on the presence of more organized F-actin structures, whereas astrocytes in substrates softer than 1kPa tended to remain as round bodies.

The main limitation observed in both systems was the decrease in expression of phenotypical morphologies observed from Day 5 to Day 10 post-encapsulation. One possible cause is that the degradation rate was fast enough to deprive cells from attachment points. However, the limited access to nutrients upon serum removal could be a confounding factor. Although the degree of cellular expansion decreased as the hydrogels degrade, future studies are required to assess the effect of an *in vivo* environment where extracellular fluid, as the main factor of degradation, is expected to be limited. It is possible that hydrogel functional groups will require modification to alter the degradation rate and allow cells to develop within the constrained fluid flow conditions present upon *in vivo* implantation.

ECM molecules influence cellular behaviour and control neural stem cell differentiation as they migrate and develop into mature neurons or glia [49, 50]. In particular, laminin [51] and collagen-IV [52, 53] are critical for development of neurons in PNS [45]. It was found that SCs within the 3D hydrogel environment expressed both laminin and collagen-IV. This expression was expected as previous reports have found that laminin and collagen-IV are the major constituents of SC ECM [53, 54]. Increased expression of laminin has been regarded as an element to promote enhanced axonal growth [55]. As shown in Figure 6B the highest expression of laminin occurred in 10 wt% hydrogels when substrate stiffness was close to 1 kPa (an average neural environment). It is possible that the enhanced laminin expression in 10 wt% hydrogels was due to cells being presented with a 1 kPa modulus for longer periods than cells in 5 wt% hydrogels. This mechanical modulus mediated impact on laminin expression has also been observed by Ning *et al.* [56] where laminin expression increased ~2 times when SCs were cultured in alginate hydrogels with stiffness of 1.17 kPa in comparison with cells cultured within 6 kPa - 10 kPa gels. An important implication of this finding is that neurons preferentially extend longer neurites when grown on ~1kPa substrates [11, 14, 57]. As such it is expected that SCs encapsulated within 10 wt% PVA-SG should be able to promote an enhanced neurite outgrowth result through a combined effect from substrate mechanical modulus and an increase in laminin expression.

Previous reports have shown that collagen-IV up regulation is indicative of a cellular response to nerve injury [58]. It has also been reported that *in vivo* collagen-IV is mainly present in the perineurium and that collagen fibrils provide the perineurium with its tensile strength [17]. It is suggested that the increased expression of collagen-IV may be a cellular response to physically restore cellular milieu. However, high levels of expression were only sustained in 10 wt% hydrogels. Since 5 wt% gels degraded faster than 10 wt%, this suggests that cells may require a longer degradation rate to allow an appropriate ECM assembly to replace the degrading network.

In this study there were no chemical factors stimulating cell growth, alignment or migration nor overload of ECM components, such as fibronectin influencing cellular responses. As such the physical property of substrate stiffness was the dominant factor influencing SC morphology. These studies indicate that 10 wt% PVA-SG gels are preferable for supporting SCs in 3D neural tissue engineering than 5 wt% PVA-SG gels. However, the ability of SCs to adapt to the environment suggests that the addition of neural cells within the hydrogel may impact on these findings. Furthermore, the use of media to support these cells *in vitro* is a confounding factor that is difficult to assess when considering that these scaffolds are intended to be supported within an *in vivo* environment. While SC responses *in vivo* are beyond the scope of this study, the impact of co-culture with neural cells was an important next step.

As expected, encapsulated cells in co-culture were found to have a higher cellular viability at Day 2 and Day 5 (>90%) in comparison with standalone SC encapsulation studies (80%-84%). This impact on cellular viability was most likely due to the presence of growth factors that are known to be provided by contact with neurons [59]. This degree of support was also observed by an increase in cellular density. While standalone SC density decreased to 20% by Day 5, SC in co-culture with PC12 cells were found to increase (1.7 fold) and maintain a constant cellular density throughout study period (Figure 7B). Since cell culture conditions were shifted from proliferation (high serum) to differentiation (low serum) at 3 Days post-encapsulation, there were no exogenous growth factors that could explain the increase in SC population other than mitogenic factors provided by PC12 cells, a phenomena that has been observed when co-culturing dorsal root ganglion cells with SCs [44]. Although further studies are required to decouple the metabolic activity contribution of each cell type, this increase in metabolic activity is most likely due to PC12 differentiation and consequent neurite outgrowth. This was further supported by assessing β-III tubulin expression associated with neurite outgrowth of encapsulated PC12 cells with SCs in comparison with encapsulated standalone PC12 cells.

PC12 cells have been used to study neuronal differentiation and explore the function of sympathetic neurons [60, 61]. Specifically, PC12 cells represent the last stage of sympathetic neuron development characterised by differentiation of sympathetic neural progenitors into post-mitotic sympathetic neurons [60, 61]. Previous studies suggest that a starvation of mitogen nutrients in the media, forcing neural progenitors to extend processes and innervate target cells, triggers this event [38-40]. Upon innervation, target cells synthesise and supply neurons with NGF by retrograde axonal transport [62]. Since sympathetic neurons depend on NGF to differentiate and survive, populations of neurons that fail to innervate a target organ degrade and eventually die [38, 39]. During this process SCs provide sympathetic neurons with trophic factors and a substrate rich in ECM molecules, where the most abundant are laminin and collagen-IV [46]. Likewise, outgrowing peripheral nerves provide SCs with mitogenic factors that support glia proliferation in development and nerve injury [44]. This mutually supportive phenomenon is representative of functional neuron and glia co-cultures during both neuronal development and nerve injury repair [44, 46].

In vitro, PC12 cells can be used to reproduce this scenario by providing a substrate rich in laminin or collagen-IV, reducing serum in media and supplementing cultures with NGF. This can also be achieved by co-culturing neurons with their respective glia. However, while neuron/glia co-cultures have been shown effective on 2D substrates [63-68], traditional cell layering techniques where glial cells are allowed to reach confluence followed by seeding neuronal cell lines, are limited in that 3D encapsulation requires simultaneous incorporation of both cell types cultured in same nutrient mix and signalling factors. In this study it is shown that, using PC12 cells and SCs in simultaneous encapsulation within PVA-SG hydrogels, the mutually supportive phenomenon can be recapitulated presented as the increase in neurite outgrowth together with the enhanced metabolic activity and the increase in SC number. Furthermore, the most remarkable result was SCs ability of extending a 3D cellular matrix inside the hydrogel 8 Days post-encapsulation, which presented PC12 cells with a substrate to extend neurites. This neurite network was decorated with laminin and collagen-IV

produced by SCs. Overall, this is a clear indication that the PVA-SG microenvironment allows SCs to physically and biochemically support neurite outgrowth.

The degree of association into neuronal networks was comparable with a similar study conducted on encapsulated primary tissue explants [18]. While Suri *et al.* [18] found that SCs and DRG neurons associate into neuronal networks when simultaneously encapsulated in a collagen/hyaluronic acid/laminin hydrogel, the abundant presence of ECM components limit the ability to assess whether neuronal development is promoted by SCs or by ECM molecules. In contrast, the present work shows that SCs were able to support PC12 development without the inclusion of exogenous ECM molecules based on the hypotheses that neuronal support can be better promoted by the incorporation of accessory cells, which were supported by the physical properties of PVA-SG hydrogels. One disadvantage of the current approach is that it requires NGF supplementation to allow for PC12 survival and differentiation. Further research will assess a more responsive non-trophic dependent primary neuroprogenitor model.

The significance of these results is that PVA-SG hydrogels can be used as a platform to reproduce cell culture techniques that are representative of *in vivo* nerve tissue regeneration. Furthermore, the backbone chemistry of PVA-SG hydrogel enables for seamless integration with conductive hydrogel technologies that are used as a substrate in the emerging field of living bioelectronics [34, 69, 70].

5. Conclusions

SCs are clearly an essential component for development of functional neural networks in 3D using PC12 cells. SCs are known to present with very different phenotypes that can be inferred from morphological characteristics. It was found that SCs dynamically respond to PVA-SG stiffness, with changes in ECM expression that were dependant on the mechanical moduli of the degrading hydrogel. These findings, supported by literature, suggest that glial cells are better supported within the stiffer 10 wt% hydrogel. The main limitation observed was the decrease in cytoplasmic

extensions and expression of phenotypical morphologies as the hydrogel degrades. While a fast degradation rate could be depriving cells from physical support, this limitation could be addressed by slowing the degradation rate of the hydrogel scaffold by increasing the number of crosslinking groups per PVA chain.

SCs were simultaneously encapsulated with PC12 cells to assess the required conditions that promote SC support of neuronal-like cells into networks. SCs and PC12 cells successfully associated into networks within 10% PVA-SG hydrogel. Further research will assess the PVA-SG potential to enable formation of functional neuronal networks with tissue cultures such as stem cells or primary tissue explants to better mimic in vivo cell behaviours, in particular, the ability of establishing functional synaptic connections with target tissue. It is also essential to assess the impact of a mechanically constrained environment with an uncertain access to nutrients, resembling conditions presented to implanted devices *in vivo*. In parallel, further exploration on hydrogel scaffolds topography is required to promote cellular alignment to direct neurite outgrowth towards target tissue.

Acknowledgements
The authors acknowledge funding from University of New South Wales and The Australian Research Council through its Special Research Initiative (SRI) in Bionic Vision Science

Received: ((will be filled in by the editorial staff))
Revised: ((will be filled in by the editorial staff))
Published online: ((will be filled in by the editorial staff))

References

[1] K.Y. Lee, D.J. Mooney, Hydrogels for Tissue Engineering, Chemical Reviews 101(7) (2001) 1869-1880.
[2] A.S. Hoffman, Hydrogels for biomedical applications, Advanced Drug Delivery Reviews 54(1) (2002) 3-12.
[3] F. Brandl, F. Sommer, A. Goepferich, Rational design of hydrogels for tissue engineering: Impact of physical factors on cell behavior, Biomaterials 28(2) (2007) 134-146.
[4] J.L. Drury, D.J. Mooney, Hydrogels for tissue engineering: scaffold design variables and applications, Biomaterials 24(24) (2003) 4337-4351.

[5] S.M. Willerth, K.J. Arendas, D.I. Gottlieb, S.E. Sakiyama-Elbert, Optimization of fibrin scaffolds for differentiation of murine embryonic stem cells into neural lineage cells, Biomaterials 27(36) (2006) 5990-6003.
[6] K. Franze, P.A. Janmey, J. Guck, Mechanics in Neuronal Development and Repair, Annual Review of Biomedical Engineering 15(1) (2013) 227-251.
[7] W. Zhou, J.M. Stukel, H.L. Cebull, R.K. Willits, Tuning the Mechanical Properties of Poly(Ethylene Glycol) Microgel-Based Scaffolds to Increase 3D Schwann Cell Proliferation, Macromolecular bioscience 16(4) (2016) 535-544.
[8] D.D. Dewitt, S.N. Kaszuba, D.M. Thompson, J.P. Stegemann, Collagen I-Matrigel Scaffolds for Enhanced Schwann Cell Survival and Control of Three-Dimensional Cell Morphology, Tissue Engineering Part A 15(10) (2009) 2785-2793.
[9] C. Lopez-Fagundo, E. Bar-Kochba, L.L. Livi, D. Hoffman-Kim, C. Franck, Three-dimensional traction forces of Schwann cells on compliant substrates, Journal of the Royal Society, Interface / the Royal Society 11(97) (2014).
[10] Y. Gu, Y. Ji, Y. Zhao, Y. Liu, F. Ding, X. Gu, Y. Yang, The influence of substrate stiffness on the behavior and functions of Schwann cells in culture, Biomaterials 33(28) (2012) 6672-6681.
[11] A.P. Balgude, X. Yu, A. Szymanski, R.V. Bellamkonda, Agarose gel stiffness determines rate of DRG neurite extension in 3D cultures, Biomaterials 22(10) (2001) 1077-1084.
[12] R.K. Willits, S.L. Skornia, Effect of collagen gel stiffness on neurite extension, Journal of Biomaterials Science, Polymer Edition 15(12) (2004) 1521-1531.
[13] J.B. Leach, X.Q. Brown, J.G. Jacot, P.A. Dimilla, J.Y. Wong, Neurite outgrowth and branching of PC12 cells on very soft substrates sharply decreases below a threshold of substrate rigidity, J Neural Eng 4(2) (2007) 26-34.
[14] L.A. Flanagan, Y. Ju, B. Marg, M. Osterfield, P.A. Janmey, Neurite branching on deformable substrates, Neuroreport 13(18) (2002) 2411-5.
[15] N.J. Allen, B.A. Barres, Neuroscience: Glia - more than just brain glue, Nature 457(7230) (2009) 675-677.
[16] D.M. Thompson, H.M. Buettner, Neurite Outgrowth Is Directed by Schwann Cell Alignment in the Absence of Other Guidance Cues, Annals of Biomedical Engineering 34(1) (2006) 161-168.
[17] N. Kleitman, R.P. Bunge, The Schwann cell: morphology and development, The Axon: Structure, Function and Pathophysiology, Oxford University Press, New York, Oxford (1995) 97-115.
[18] S. Suri, C.E. Schmidt, Cell-laden hydrogel constructs of hyaluronic acid, collagen, and laminin for neural tissue engineering, Tissue Engineering - Part A 16(5) (2010) 1703-1716.
[19] J.M. Edgar, M. Robinson, S.M. Willerth, Fibrin hydrogels induce mixed dorsal/ventral spinal neuron identities during differentiation of human induced pluripotent stem cells, Acta Biomaterialia 51 (2017) 237-245.
[20] K.J. Lampe, A.L. Antaris, S.C. Heilshorn, Design of three-dimensional engineered protein hydrogels for tailored control of neurite growth, Acta Biomaterialia 9(3) (2013) 5590-5599.
[21] R. Lozano, L. Stevens, B.C. Thompson, K.J. Gilmore, R. Gorkin, E.M. Stewart, M. in het Panhuis, M. Romero-Ortega, G.G. Wallace, 3D printing of layered brain-like structures using peptide modified gellan gum substrates, Biomaterials 67 (2015) 264-273.
[22] A. Banerjee, M. Arha, S. Choudhary, R.S. Ashton, S.R. Bhatia, D.V. Schaffer, R.S. Kane, The influence of hydrogel modulus on the proliferation and differentiation of encapsulated neural stem cells, Biomaterials 30(27) (2009) 4695-4699.
[23] C.T.S. Wong Po Foo, J.S. Lee, W. Mulyasasmita, A. Parisi-Amon, S.C. Heilshorn, Two-component protein-engineered physical hydrogels for cell encapsulation, Proceedings of the National Academy of Sciences 106(52) (2009) 22067.
[24] T.-Y. Cheng, M.-H. Chen, W.-H. Chang, M.-Y. Huang, T.-W. Wang, Neural stem cells encapsulated in a functionalized self-assembling peptide hydrogel for brain tissue engineering, Biomaterials 34(8) (2013) 2005-2016.
[25] W. Sun, T. Incitti, C. Migliaresi, A. Quattrone, S. Casarosa, A. Motta, Viability and neuronal differentiation of neural stem cells encapsulated in silk fibroin hydrogel functionalized with an IKVAV peptide, Journal of Tissue Engineering and Regenerative Medicine (2015) n/a-n/a.

[26] H. Li, A. Wijekoon, N.D. Leipzig, Encapsulated neural stem cell neuronal differentiation in fluorinated methacrylamide chitosan hydrogels, Annals of Biomedical Engineering 42(7) (2014) 1456-1469.
[27] C. Chung, K.J. Lampe, S.C. Heilshorn, Tetrakis(hydroxymethyl) Phosphonium Chloride as a Covalent Cross-Linking Agent for Cell Encapsulation within Protein-Based Hydrogels, Biomacromolecules 13(12) (2012) 3912-3916.
[28] D.D. McKinnon, A.M. Kloxin, K.S. Anseth, Synthetic hydrogel platform for three-dimensional culture of embryonic stem cell-derived motor neurons, Biomaterials Science 1(5) (2013) 460-469.
[29] S. Koutsopoulos, S. Zhang, Long-term three-dimensional neural tissue cultures in functionalized self-Assembling peptide hydrogels, Matrigel and Collagen i, Acta Biomaterialia 9(2) (2013) 5162-5169.
[30] M.J. Mahoney, K.S. Anseth, Three-dimensional growth and function of neural tissue in degradable polyethylene glycol hydrogels, Biomaterials 27(10) (2006) 2265-2274.
[31] K.S. Lim, Y. Ramaswamy, J.J. Roberts, M.-H. Alves, L.A. Poole-Warren, P.J. Martens, Promoting Cell Survival and Proliferation in Degradable Poly(vinyl alcohol)–Tyramine Hydrogels, Macromolecular bioscience 15(10) (2015) 1423-1432.
[32] U.A. Aregueta-Robles, P.J. Martens, L.A. Poole-Warren, R.A. Green, Tailoring 3D hydrogel systems for neuronal encapsulation in living electrodes, Journal of Polymer Science Part B: Polymer Physics 56(4) (2018) 273-287.
[33] L.A. Flanagan, Y.E. Ju, B. Marg, M. Osterfield, P.A. Janmey, Neurite branching on deformable substrates, Neuroreport 13(18) (2002) 2411-5.
[34] J. Goding, A. Gilmour, U.A. Robles, L. Poole-Warren, N. Lovell, P. Martens, R. Green, A living electrode construct for incorporation of cells into bionic devices, MRS Communications 7(3) (2017) 487-495.
[35] B. Halliwell, S. Chirico, Lipid peroxidation: its mechanism, measurement, and significance, The American Journal of Clinical Nutrition 57(5) (1993) 715S-724S.
[36] S.J. Bryant, K.S. Anseth, Hydrogel properties influence ECM production by chondrocytes photoencapsulated in poly(ethylene glycol) hydrogels, Journal of Biomedical Materials Research 59(1) (2002) 63-72.
[37] P.C. Georges, W.J. Miller, D.F. Meaney, E.S. Sawyer, P.A. Janmey, Matrices with Compliance Comparable to that of Brain Tissue Select Neuronal over Glial Growth in Mixed Cortical Cultures, Biophysical Journal 90(8) (2006) 3012-3018.
[38] A.M. Davies, The Neurotrophic Hypothesis: Where does it Stand?, Philosophical Transactions of the Royal Society of London. Series B: Biological Sciences 351(1338) (1996) 389-394.
[39] R.W. Oppenheim, Cell Death During Development of the Nervous System, Annual Review of Neuroscience 14(1) (1991) 453-501.
[40] R. Levi-Montalcini, The nerve growth factor: thirty-five years later, Bioscience reports 7(9) (1987) 681-699.
[41] D.E. Syroid, P.R. Maycox, P.G. Burrola, N. Liu, D. Wen, K.-F. Lee, G. Lemke, T.J. Kilpatrick, Cell death in the Schwann cell lineage and its regulation by neuregulin, Proceedings of the National Academy of Sciences 93(17) (1996) 9229-9234.
[42] E.M. Eves, L.H. Boise, C.B. Thompson, A.J. Wagner, N. Hay, M.R. Rosner, Apoptosis Induced by Differentiation or Serum Deprivation in an Immortalized Central Nervous System Neuronal Cell Line, Journal of Neurochemistry 67(5) (1996) 1908-1920.
[43] J.L. Salzer, R.P. Bunge, L. Glaser, Studies of Schwann cell proliferation. III. Evidence for the surface localization of the neurite mitogen, Journal of cell biology 84(3) (1980) 767-778.
[44] P.M. Wood, R.P. Bunge, Evidence that sensory axons are mitogenic for Schwann cells, Nature 256(5519) (1975) 662-664.
[45] D.J. Carey, R.P. Bunge, Factors influencing the release of proteins by cultured schwann cells, The Journal of Cell Biology 91(3) (1981) 666-672.
[46] R.P. Bunge, Expanding roles for the Schwann cell: ensheathment, myelination, trophism and regeneration, Current Opinion in Neurobiology 3(5) (1993) 805-809.
[47] P.K. Thomas, Changes in the endoneurial sheaths of peripheral myelinated nerve fibres during Wallerian degeneration, Journal of Anatomy 98(Pt 2) (1964) 175-182.
[48] K.R. Jessen, R. Mirsky, The origin and development of glial cells in peripheral nerves, Nat Rev Neurosci 6(9) (2005) 671-682.

[49] C.S. Barros, S.J. Franco, U. Müller, Extracellular Matrix: Functions in the nervous system, Cold Spring Harbor Perspectives in Biology 3(1) (2011) 1-24.
[50] J.R. Sanes, Extracellular Matrix Molecules that Influence Neural Development, Annual Review of Neuroscience 12(1) (1989) 491-516.
[51] J.L. Podratz, E. Rodriguez, A.J. Windebank, Role of the extracellular matrix in myelination of peripheral nerve, Glia 35(1) (2001) 35-40.
[52] D.J. Carey, M.S. Todd, Schwann cell myelination in a chemically defined medium: demonstration of a requirement for additives that promote Schwann cell extracellular matrix formation, Developmental Brain Research 32(1) (1987) 95-102.
[53] C.F. Eldridge, M.B. Bunge, R.P. Bunge, P.M. Wood, Differentiation of axon-related Schwann cells in vitro. I. Ascorbic acid regulates basal lamina assembly and myelin formation, The Journal of Cell Biology 105(2) (1987) 1023-1034.
[54] D.J. Carey, C.F. Eldridge, C.J. Cornbrooks, R. Timpl, R.P. Bunge, Biosynthesis of type IV collagen by cultured rat Schwann cells, The Journal of cell biology 97(2) (1983) 473-479.
[55] X. Xu, N. Geremia, F. Bao, A. Pniak, M. Rossoni, A. Brown, Schwann Cell Coculture Improves the Therapeutic Effect of Bone Marrow Stromal Cells on Recovery in Spinal Cord-Injured Mice, Cell transplantation 20(7) (2011) 1065-1086.
[56] L. Ning, Y. Xu, X. Chen, D.J. Schreyer, Influence of mechanical properties of alginate-based substrates on the performance of Schwann cells in culture, Journal of Biomaterials Science, Polymer Edition 27(9) (2016) 898-915.
[57] D. Koch, William J. Rosoff, J. Jiang, Herbert M. Geller, Jeffrey S. Urbach, Strength in the Periphery: Growth Cone Biomechanics and Substrate Rigidity Response in Peripheral and Central Nervous System Neurons, Biophysical Journal 102(3) (2012) 452-460.
[58] J. Siironen, M. Sandberg, V. Vuorinen, M. Röyttä, Laminin B1 and Collagen Type IV Gene Expression in Transected Peripheral Nerve: Reinnervation Compared to Denervation, Journal of Neurochemistry 59(6) (1992) 2184-2192.
[59] S. Fu, T. Gordon, The cellular and molecular basis of peripheral nerve regeneration, Mol Neurobiol 14(1-2) (1997) 67-116.
[60] K. Fujita, P. Lazarovici, G. Guroff, Regulation of the differentiation of PC12 pheochromocytoma cells, Environmental Health Perspectives 80(0091-6765 (Print)) (1989) 15.
[61] L.A. Greene, A.S. Tischler, PC12 Pheochromocytoma cultures in neurobiological research, Advances in cellular neurobiology 3 (1982) 40.
[62] S. Korsching, H. Thoenen, Nerve growth factor in sympathetic ganglia and corresponding target organs of the rat: correlation with density of sympathetic innervation, Proceedings of the National Academy of Sciences of the United States of America 80(11) (1983) 3513-3516.
[63] M. Cochran, M.M. Black, PC12 neurite regeneration and long-term maintenance in the absence of exogenous nerve growth factor in response to contact with Schwann cells, Developmental Brain Research 17(1–2) (1985) 105-116.
[64] M.F.B. Daud, K.C. Pawar, F. Claeyssens, A.J. Ryan, J.W. Haycock, An aligned 3D neuronal-glial co-culture model for peripheral nerve studies, Biomaterials 33(25) (2012) 5901-5913.
[65] D. Majumdar, Y. Gao, D. Li, D.J. Webb, Co-culture of neurons and glia in a novel microfluidic platform, Journal of Neuroscience Methods 196(1) (2011) 38-44.
[66] H.-p. Xu, L. Gou, H.-W. Dong, Study Glial Cell Heterogeneity Influence on Axon Growth Using a New Coculture Method, (43) (2010) e2111.
[67] E. Goto, M. Mukozawa, H. Mori, M. Hara, A rolled sheet of collagen gel with cultured Schwann cells: Model of nerve conduit to enhance neurite growth, Journal of Bioscience and Bioengineering 109(5) (2010) 512-518.
[68] K.H. Adcock, D.J. Brown, M.C. Shearer, D. Shewan, M. Schachner, G.M. Smith, H.M. Geller, J.W. Fawcett, Axon behaviour at Schwann cell - Astrocyte boundaries: Manipulation of axon signalling pathways and the neural adhesion molecule L1 can enable axons to cross, European Journal of Neuroscience 20(6) (2004) 1425-1435.

[69] R.A. Green, R.T. Hassarati, J.A. Goding, S. Baek, N.H. Lovell, P.J. Martens, L.A. Poole-Warren, Conductive hydrogels: mechanically robust hybrids for use as biomaterials, Macromolecular bioscience 12(4) (2012) 494-501.
[70] U.A. Aregueta-Robles, A.J. Woolley, L.A. Poole-Warren, N.H. Lovell, R.A. Green, Organic electrode coatings for next-generation neural interfaces, Frontiers in neuroengineering 7 (2014) 15.

Supplementary Material

Click here to download Supplementary Material: Acta_Biom_Supplementary data.docx

Supplementary Material

Click here to download Supplementary Material: Video1 - SC_PC12 2DIV SCs-Green PC12-Red Nuclei-Blue.mpg

Supplementary Material

Click here to download Supplementary Material: Video2 - SC_PC12 5DIV SCs-Green PC12-Red Nuclei-Blue.mpg

Supplementary Material

Click here to download Supplementary Material: Video3 - SC_PC12 8DIV SCs-Green PC12-Red Nuclei-Blue.mpg

Supplementary Material

Click here to download Supplementary Material: Video4 - SC_PC12 8DIV SCs-Green PC12-Red Nuclei-Blue.mpg

Supplementary Material

Click here to download Supplementary Material: Video5 - SC_PC12 8DIV SCs-Green PC12-Red Nuclei-Blue.mpg